Plant Biology ISSN 1435-8603

RESEARCH PAPER

The mode of interaction between *Vitis* and *Plasmopara viticola* Berk. & Curt. Ex de Bary depends on the host species

G. Jürges[1], H.-H. Kassemeyer[2], M. Dürrenberger[3], M. Düggelin[3] & P. Nick[1]

1 Institute of Botany 1, University of Karlsruhe, Karlsruhe, Germany
2 State Institute for Viticulture and Oenology, Freiburg, Germany
3 Centre of Microscopy, Biozentrum/Pharmazentrum, University of Basel, Basel, Switzerland

Keywords
Coevolution; guard cells; host–pathogen interaction; resistance.

Correspondence
P. Nick, Botanisches Institut 1, Universität Karlsruhe, Kaiserstr. 2, 76128 Karlsruhe, Germany.
E-mail: peter.nick@bio.uni-karlsruhe.de

Editor
N. van Dam

Received: 18 August 2008; Accepted: 13 November 2008

doi:10.1111/j.1438-8677.2008.00182.x

ABSTRACT

In order to obtain insight into host responses to grapevine downy mildew (*Plasmopara viticola*), we compared pathogen development on a panel of *Vitis* species from North America, Asia and Europe. Leaf discs from different host species were inoculated in parallel, and the colonisation of the mesophyll was visualised by aniline blue staining and quantified with respect to infection incidence and mycelial growth. In parallel, the morphology of guard cells was screened for the presence of an internal cuticular rim after staining with acridine orange and using low-temperature scanning electron microscopy. We observed three response patterns: (i) inhibition of pathogen development early after attachment of zoospores; (ii) successful colonisation of the mesophyll by the pathogen; and (iii) aberrant development, where the pathogen does not attach to guard cells, but produces hyphae on the leaf surface without formation of viable sporangiophores. Inhibition is observed in the North American and Siberian species, successful colonisation prevails in the European hosts, and surface hyphae are found on non-Siberian Asiatic species. We propose that the interaction between host and pathogen is under control of specific signals that have been subject to evolutionary diversification.

INTRODUCTION

The grapevine pathogen *Plasmopara viticola* originally infected wild species of *Vitis* in North America, but invaded Europe in the 1870s, where it infected the previously unexposed host cultivars of *Vitis vinifera* and soon developed into a major problem in vineyards throughout the continent. Since then, it has caused extensive losses in yield due to infection of leaves, inflorescences and clusters. Especially at high humidity, it can spread rapidly over large areas within a very short period of time (Müller & Sleumer 1934). The first pathogen inoculum in spring derives from overwintering sexual oospores (Vercesi *et al.* 1999). It is, however, the rapid sequence of asexual propagation by sporangia under optimal conditions, such as high humidity and warm temperatures, that causes severe epidemics and renders *P. viticola* a serious threat to viticulture (Müller & Sleumer 1934).

The lemon-shaped sporangia are coenocytic and contain four to eight nuclei (Riemann *et al.* 2002). Upon contact with water, they release several flagellate zoospores that swarm within the water film on the lower surface of the leaf. On susceptible hosts, the zoospores are targeted to the stomata, where they shed their flagella, attach and encyst (Kiefer *et al.* 2002). Subsequently, they form a germ tube that reaches into the substomatal cavity, where it dilates into a substomatal vesicle. From this substomatal vesicle, a primary hypha emerges, and develops a mycelium that spreads within the leaf tissue, extending mainly into the intercellular spaces of the spongy parenchyma and forming haustoria that penetrate into the cell wall of the host (Unger *et al.* 2007).

A comparison of early development between a host-free system (Riemann *et al.* 2002) and a biotic system based on leaf discs (Kiefer *et al.* 2002) revealed host factors promote and control early stages of the infection cycle, especially the hatching of *P. viticola* zoospores from the sporangia, and the morphogenesis of the germ tube. In addition, it was demonstrated that the zoospores track the stomata actively and are guided by host factors that are released from open stomata (Kiefer *et al.* 2002). The nature of these host factors in the *Vitis–P. viticola* pathosystem remains to be elucidated.

Historical evidence strongly suggests that *P. viticola* originated in North America, where it is thought to have originally co-evolved with native *Vitis* species. In Asia, *P. viticola* is not known, but related species such as *Plasmopara cissii* and *Plasmopara amurensis* (Grünzel 1959; Dick 2002) have presumably coevolved with the Vitaceae species native to their range of distribution. In Europe, *Vitis* evolved in the absence of *Plasmopara* species that can infect grapevines. Thus, the host factors that regulate pathogen development are expected to be subject to evolutionary change. We therefore investigated and compared guard cell morphology and the initial stages of attempted infection (in leaf discs) by *P. viticola* in different *Vitis* species from North America, Asia and Europe.

MATERIALS AND METHODS

Plant material

The plant material used in this study originated from several sources, including the Institute of Viticulture of the State of Baden-Württemberg, the USDA National Clonal Germplasm Repository, University of California-Davis (USA), the *Vitis* collection at the Julius-Kühn Institute, Geilweiler Hof, Siebeldingen (Germany) and the Botanical Gardens of Bayreuth and Lublin. All specimens were verified morphologically and by molecular markers for their identity and are maintained as reference in the collection of the Botanical Garden of the University of Karlsruhe. We used *Vitis vinifera* cv. Müller-Thurgau, a white-fruited grape cultivar widely grown throughout Central Europe that is susceptible to infection by *P. viticola*, as a representative of cultivated grapevines of this species. Together with *V. vinifera* ssp. *sylvestris* (accession Ketsch, in the following termed *V. sylvestris* Ketsch), the only wild taxon of *Vitis* occurring in Europe, this constituted the European part of the species collection. *Vitis amurensis* (Siberia), *Vitis coignetiae* (Korea, Manchuria), *Vitis ficifolia* (Japan, China), *Vitis quinquangularis* (China) and *Vitis jacquemontii* (Pakistan) were chosen as Asian species; while *Vitis rupestris* (south-eastern USA), *Vitis riparia* (north-eastern USA) and *Vitis californica* (west coast USA) were used to represent North American species. The natural distributions of these accessions are shown in Fig. 1. Additionally, *Vitis* hybrid cv. Merzling, a progeny of complex pseudo-backcrosses with *V. vinifera* cultivars and *V. vinifera* × American species hybrids were included in the experiments. Cuttings of these species were cultivated in a greenhouse in pots on soil under natural light supplemented in a 16 h:8 h light:dark cycle by artificial daylight (400 W, Vialox NAV-T, SON-T; Osram, Mühlheim, Germany).

Pathogen material

For the inoculation experiments, a mixed source culture of *P. viticola* obtained from various natural field populations collected near Freiburg (Germany) was used. The pathogen was maintained on susceptible *V. vinifera* cv. Müller-Thurgau in a greenhouse. Periodically, the abaxial surfaces of young leaves were inoculated with a aqueous

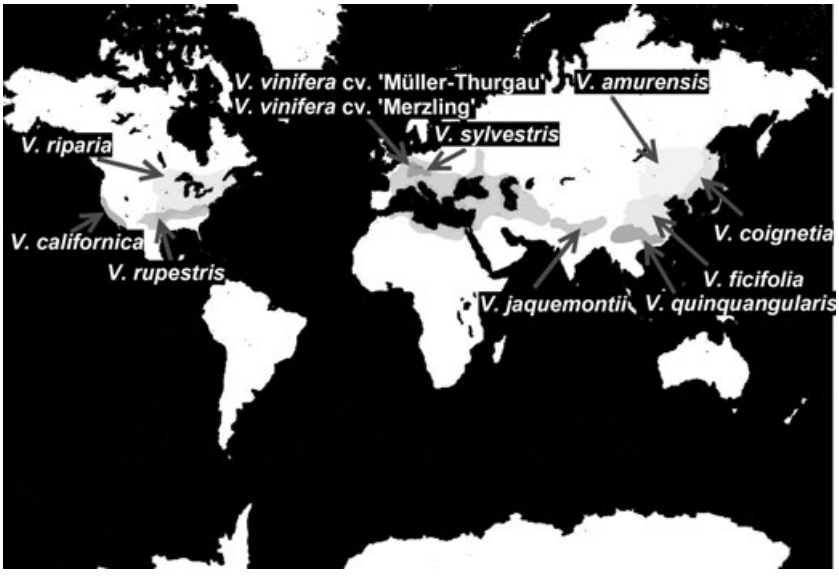

Fig. 1. Geographic distribution of the different *Vitis* species used in this study (source http://www.ars-grin.gov/npgs).

suspension containing approximately 2×10^4 sporangia ml^{-1} and kept overnight under high relative humidity (RH > 96%) at 24 °C. After incubation for 5–6 days under ambient greenhouse conditions, the plants were again maintained overnight under moist conditions to induce sporulation. Formed sporangia were harvested and used for the next inoculation series. The harvested sporangia were frozen in dry ice and stored at −20 °C until use for the next inoculation series (Riemann *et al.* 2002). The sporangia maintained full viability for up to 6 months. To verify the genetic identity of the source culture used in this study, genomic DNA was extracted from sporulating specimens, and the NL and LR regions of the large subunit of the 25–28S RNA was used as molecular marker to compare other samples of *P. viticola* collected at different sites in Europe and North America (S. Schröder, W. Wilcox & P. Nick, unpublished data). The genetic identity of mycelia formed on the infected leaves was verified at regular intervals by comparing the NL and LR sequences with those of the source culture.

Inoculation procedure

The sixth unfolded leaf (counted from the apex) was excised, surface-sterilized with 70% ethanol, rinsed with distilled water and carefully dried with household tissue. Leaf discs 14 mm in diameter were excised from fully expanded leaves such that they did not contain major veins and were placed top-down on water agar (0.8% w/v). Then, a portion of frozen sporangia was resuspended in water and adjusted to 8×10^4 sporangia·ml^{-1} using a hemacytometer (Fuchs-Rosenthal, Thoma, Freiburg, Germany), and 100 µl of this suspension were spread with a micropipette onto the leaf disc for inoculation. After inoculation, the leaf discs were incubated at 25 °C under continuous white light (5000 Lx·m^{-2}) for 72 h, when infections were analysed. To test for potential contamination of the leaf discs by other fungi, other leaf discs were incubated and similarly examined. To exclude that the inoculum was contaminated by other fungi, only sporangia derived from defined primary inocula were used. In one set of experiments, the effect of an inoculum obtained from infected grape plantlets that had been axenically raised and then infected was compared to that of an inoculum obtained as described above.

Staining of infection structures with aniline blue

To visualise the formation of hyphae on inoculated leaf discs, we used the protocol of Kiefer *et al.* (2002). In this protocol, leaf discs (diameter 10 mm) are depigmented by 10 min autoclaving at 121 °C and 120 kPa in 1 M KOH prior to staining with aniline blue (Sigma-Aldrich, Deisenhofen, Germany). Depending on the species, residual chlorophyll autofluorescence was sometimes observed, but this neither interfered with the quantification protocol (see below) nor did it impair the visibility of the aniline blue staining. After depigmentation, the leaf discs were incubated for 5 min with 0.05% w/v aniline blue in 0.067 M K_2HPO_4 (pH 9.8), washed twice for 5 min with distilled water, and then directly viewed under an epifluorescence microscope (Axioskop, Zeiss, Göttingen, Germany) using the GFP-specific filter set 13 (excitation 470 ± 20 nm, beam splitter 495 nm, and emission through a band pass filter, 505–530 nm). From each leaf disc, five images were recorded in the centre and at four equidistant points (distance to the centre: 3.00 mm) in the four main directions, using a 20× Neofluar objective (Zeiss, Göttingen, Germany). Since the view field was 3.00 mm in diameter, these images covered approximately 80% of the disc area, but did not overlap. In samples with surface mycelium, the images were recorded on two focal planes, either on the surface or about 100 µm within the tissue to assess penetration through the stomata. However, at a given infection site, there was either mycelium on the surface of the leaf without colonisation of the mesophyll or colonisation of the mesophyll without any mycelium on the surface.

Assessment of host tissue colonisation

To separate background residual chlorophyll from the aniline blue signal, the images were processed using Photoshop software (Adobe Systems Inc., USA). The images (in the format Red–Blue–Green, RGB) were split into the individual channels, and the blue channel was subjected to the autocontrast command (producing pixel intensity distributions that were comparable between different images), and the red and green channels were reduced to 0%. The result was transformed into a grey scale and subjected to the auto-grey value command, ensuring that any aniline blue signal, irrespective of its original intensity, was scored with the same pixel intensity. The processed images were analysed using the Scion Image software (Scion Corporation, Frederick, MD, USA). The individual intercostal fields were selected using the freehand tool and analysed with respect to area and integrated density of *P. viticola* mycelium. As a measure of the frequency of infection events, the area of infected intercostal fields (*i.e.* the area delineated by leaf veins) was determined as a percentage of the total area of the intercostal fields within the viewed image. Because of the low magnification, the geometry of the leaf surface remained visible as reference even when focused into the mesophyll layers. To assess the colonisation intensity of a given infection, the total projected area of mycelia within the mesophyll was determined. This was possible by measuring the integrated density within a given intercostal field, since, due to the image processing, all pixels that did not originate from hyphae were black and therefore did not contribute to the integrated density, whereas all pixels originating from hyphae contributed a pixel intensity of 255. The value obtained for the integrated density was thus proportional to the total cross-area of mycelia within the analysed area. These values can therefore be used as (relative) measures of colonisation intensity. To

compare surface growth of the mycelium, the total cross-area of mycelia on the leaf surface was measured directly by selection of the (white) mycelia using the 'magic stick' tool and quantifying the selected area in pixels. Since surface growth and colonisation of the mesophyll were mutually exclusive within a given intercostal field, the quantification of cross-area could be unequivocally attributed to the colonisation mode.

Semi-thin sections and staining of host tissue with acridine orange

Small specimens of leaf tissue were fixed in 7 $g \cdot l^{-1}$ paraformaldehyde (prepared freshly in 10 mM PIPES pH 7.0) for 1 h under vacuum. The specimens were then dehydrated through an ethanol series (10%, 30% and 100%) and then infiltrated with xylol and embedded with paraffin (Roth, Karlsruhe, Germany) at 68 °C. Semithin sections of 10 μm thickness were cut with a conventional microtome, attached to chrome gelatine, and dried for 5 h. The sections were stained for 5 min with a 10 $g \cdot l^{-1}$ aqueous solution of acridine orange adjusted to pH 7. After washing with distilled water, the specimens were dried, covered with a drop of Entellan (Merck, Darmstadt, Germany) and a coverslip, and retained for later analysis. The results were analysed under an epifluorescence microscope (Axioskop, Zeiss, Göttingen, Germany) with filter set 1 (excitation 365 ± 12 nm, beam splitter 395 nm, emission through a long-pass filter at 397 nm).

Low-temperature scanning electron microscopy

The structure of stomata was examined using low-temperature scanning electron microscopy (LT-SEM) as described by Guggenheim *et al.* (1991). Fresh leaf pieces with an area of 0.8–1.0 cm^2 were excised and mounted on a specimen holder (Balzers AG; Balzers, Lichtenstein) using a low-temperature mounting medium. After cryofixation in liquid nitrogen, samples were transferred under a nitrogen atmosphere into a Balzers cryopreparation unit SCU 020 attached to a JEOL JSM 6300 scanning electron microscope (SEM). Ice crystals on the surface of the specimen were allowed to sublimate from the surface by raising the temperature to −80 °C for about 10 min. The specimens were sputter-coated with gold (20 nm) in an argon atmosphere (Müller *et al.* 1991) and transferred into the SEM under high-vacuum conditions. The samples were observed at a stage temperature of −165 °C, using an acceleration voltage between 5 and 25 kV.

Sample sizes and statistical treatment

During this study, one to three genotypes were used per accession. The experiments presented were repeated over three consecutive vegetation periods. For analysis of guard cell morphology, each accession was investigated in five to seven independent experimental series from three different vegetation periods. In each series, 20 to 50 individual leaf discs from five to 10 plants were employed. Forty to 95 individual guard cells were viewed for the presence of the inner cuticular rim. For analysis of host tissue colonisation, 7924 images (from 70 to 119 leaf discs originating from 10 to 15 plants per accession) were analysed. The average values plotted in Fig. 7 are pooled from five to seven independent infection series from three subsequent years and between five to 10 different pathogen inocula. The variables (i) infected area (as a percentage of total area), (ii) colonisation intensity (for a given infection event as a relative unit), and (iii) surface growth (as a relative unit) were analysed for the contributions of host *versus* inoculum using the non-parametrical Kruskal–Wallis test. Throughout this study, the same pathogen material was used originating from a source culture that had been originally collected from different vineyards from the region around Freiburg and was then maintained in the greenhouse as described above.

RESULTS

Guard cell morphology

An inner cuticular rim at the neck region of the substomatal cavity was present in many of the wild *Vitis* species, but was absent in *V. vinifera* cv. Müller-Thurgau and the hybrid cv. Merzling. This inner cuticular rim could be visualised in transverse leaf sections, after staining with acridine orange, as a blue-green protrusion on the inner side of the stoma (Fig. 2, white arrowheads), similar to the outer cuticular rim present in all tested *Vitis* species and cultivars (Fig. 2, white arrows). The inner cuticular rim was absent in the grapevine cultivars Müller-Thurgau (Fig. 2A) and the wild European *V. sylvestris* Ketsch (Fig. 2B), but was present in the North American species *V. riparia, V. rupestris* (Fig. 2C and D) and *V. californica* (Table 1), as well as in the Siberian species *V. amurensis* (Fig. 2E). However, the inner cuticular rim was not observed in the Asian species *V. jacquemontii* (Fig. 2F), nor in *V. coignetiae, V. ficifolia* and *V. quinquangularis* (Table 1).

Under favourable circumstances, when the section hit the median of the stoma, the inner cuticular rim could also be observed with SEM. It was clearly absent from *V. vinifera* cv. Müller-Thurgau (Fig. 3A), but visible in the stomata of the North American species *V. riparia* (Fig. 3B) and *V. rupestris* (Fig. 3C).

Interaction between *Plasmopara viticola* and *Vitis*

In assessing the responses of different *Vitis* species to pathogen attack, we were able to define three distinct response patterns described below.

Successful colonisation

Here, the pathogen penetrates through the stomata and successfully colonises the mesophyll until sporulation. This pattern was most frequent in *V. vinifera* cv.

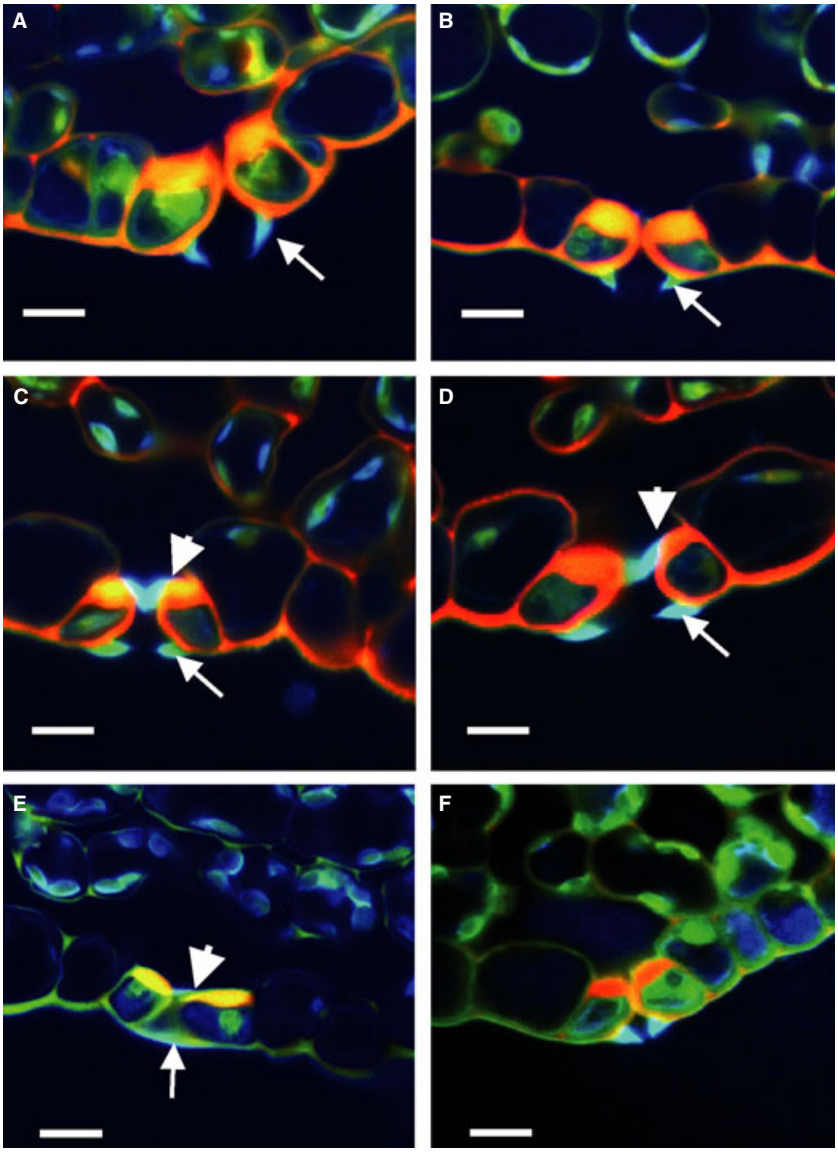

Fig. 2. Visualisation of the inner cuticular rim in leaf cross-sections from different *Vitis* species by staining with acridine orange. Sections of uninfected control leaves are shown (the presence of the inner cuticular rim is a constitutive trait independent of infection). A: grapevine cv. Müller-Thurgau, B: wild European *Vitis vinifera* ssp. *sylvestris*, C: North American *Vitis riparia*, D: *Vitis rupestris*, E: Siberian *Vitis amurensis*, F: Asian *V. jacquemontii*. White arrows indicate the outer cuticular rim present in all species, white arrowheads indicate the inner cuticular rim present only in some of the tested *Vitis* species. Size bar corresponds to 10 μm.

Müller-Thurgau, where a high number of intercostal fields were infected upon inoculation with *P. viticola*, but were also manifest, at a lower frequency, in the wild European *V. sylvestris* Ketsch (Table 1). In this response pattern, the zoospores attach close to the stomatal opening (Fig. 3D) and produce a germ tube (Fig. 3D, white arrowhead) that invades the substomatal cavity. Subsequently, a mycelium develops and rapidly penetrates the entire mesophyll (Fig. 4A–C), but only rarely crosses the veins. This can be seen most clearly during the earlier phases, when individual hyphae extend to the veins, and then bend to continue growth parallel to the vascular tissue (Fig. 4C). After a few days, arbuscular sporangiophores (Fig. 3E1–E3) emerge from the stomata. The sporangiophores branch as finer hyphae from a more solid stalk and bulge at their termini to produce the sporangia (Fig. 3E1 and E2). The finer hyphae that carry the sporangia are often intertwined with sporangiophore hyphae (Fig. 3E3). To confirm that the fine hyphae and sporangiophores were not the result of a contaminant fungus that had developed in the humid conditions of the assay, we cultivated uninoculated control discs in parallel, but did not observe hyphae or sporangiophores on these controls.

Inhibition of pathogen development

The development of the pathogen was arrested shortly after the spores had attached to the guard cells. This pattern was observed in the North American accessions *V. riparia*, *V. rupestris* (Fig. 5D and E) and *V. californica* (Table 1), but, interestingly, also in an accession from the Siberian species *V. amurensis* (Fig. 5A–C). Upon staining with aniline blue, numerous small, incomplete mycelia that were arrested at an early stage of their development (Fig. 5B and C) became visible as fluorescent dots at the

Table 1. Infection patterns and presence of the inner cuticular rim.

accession	origin	pattern	inner rim
Vitis vinifera cv. Müller-Thurgau	Germany	S	–
Vitis hybrid cv. Merzling	Germany	S, R	–
Vitis vinifera ssp. *sylvestris*	Germany	(S), Ab	–
Vitis riparia	North America	R	+
Vitis rupestris	North America	R	+
Vitis californica	North America	R	+
Vitis amurensis	Siberia	R	+
Vitis coignetiae	Korea	Ab	–
Vitis ficifolia	China	Ab	–
Vitis quinquangularis	China	Ab	–
Vitis jacquemontii	Pakistan	Ab	–

S, successful colonisation (susceptibility of the host); *R*, inhibited colonisation (resistance of the host); *Ab*, aberrant development with hyphae on the leaf surface.
The presence (+) or absence (–) of the inner cuticular rim is also indicated. *V. vinifera* cvs. Müller-Thurgau and Merzling differ genetically because cv. Merzling has been generated by a complex series of crosses and back-crosses involving wild *Vitis* species from North America.

stomata (*V. amurensis*, Fig. 5A), or, in some cases, also along leaf veins (*V. rupestris*, Fig. 5D). At higher magnification (Fig. 5B and C), these spots can be seen to represent small, incomplete mycelia that have been arrested at an early stage of development.

Surface hyphae

An extensive mycelium developed on the leaf surface without penetrating through the stomata. This pattern occurred in accessions of the East Asian species *V. ficifolia*, *V. coignetiae* and *V. quinquangularis* (Table 1) and, most spectacularly, in the Central Asian *V. jacquemontii* (Figs 3G and 6A–E). In contrast to the other two response patterns, the pathogen did not enter the stomata, but developed an extensive mycelium on the surface of the leaf. We followed the development of this mycelium over time (Fig. 6A–E) and observed that zoospores failed to track the stomata and attached at apparently random sites on the leaf surface (Fig. 6A) or often at leaf veins. From these spores, multiple germ tubes emerged (Fig. 6B and C), which developed into a mycelium that preferentially covered leaf veins or trichomes (Figs 3G white box, 6D) and, in contrast to the situation in a susceptible host (Fig. 3E), failed to develop viable sporangiophores (Fig. 3G). When control discs were incubated for the same time without inoculation, this surface mycelium was not observed (Fig. 6E, inset). To test the possibility that the surface mycelium developed from contamination of the inoculum by other fungi, we performed control inoculations using sporangia that had been harvested from plantlets cultivated under axenic conditions. When inoculated on *V. coignetiae* or *V. ficifolia*, a surface mycelium developed, whereas on the susceptible cultivar Müller-Thurgau, the same inoculum did not produce a surface mycelium, but gave the typical mesophyll colonisation pattern (data not shown). In addition, the NL and LR regions of the large subunit of the 25-28S RNA showed identity with the source inoculum (Schröder *et al.* unpublished data). A variation of this pattern was observed in the wild European *V. sylvestris* Ketsch (Fig. 6F, Table 1). In this host, most zoospores similarly developed a mycelium on the surface of the leaf. However, occasionally, successful penetration through the stomata was observed (in this case, no surface mycelium was produced in the respective intercostal field). A closer examination revealed that in these cases the zoospores had not attached to the stoma itself but had developed a long germ tube that grew directionally over a considerable distance (up to 100 μm or more) towards the nearest stoma (Fig. 3F).

These three patterns were clearly distinct; however, they were manifest to variable degrees in different species of *Vitis*. When the infected area was measured, a clear difference between genotypes of European origin and species from North America and East Asia emerged (Fig. 7A). The cv. Müller-Thurgau showed the highest values for infected area, along with the hybrid cv. Merzling, and the wild European *V. sylvestris* Ketsch, whereas values were low in the two species from North America, *V. riparia* and *V. rupestris*, and in the species from Asia. A similar, but not identical pattern was observed when the colonisation intensity of a given infection site was taken into account (Fig. 7B). Again, the highest values were obtained for the cv. Müller-Thurgau, with a strongly reduced colonisation intensity observed in the wild European *V. sylvestris* Ketsch. Interestingly, intensive colonisation of the mesophyll was virtually absent in the American species *V. riparia* and *V. rupestris*, although both species displayed low, but not negligible, values for infected area (compare Fig. 7B with Fig. 7A). Mesophyll colonisation was not observed in the Asian species, with exception of the Siberian *V. amurensis*, which was comparable to the wild European *V. sylvestris* Ketsch in both the infection area (Fig. 7A) and colonisation intensity (Fig. 7B). A clear and distinctive pattern also emerged when the extent of fungal growth on the leaf surface was scored (Fig. 7C). Interestingly, surface growth and colonisation of the mesophyll were mutually exclusive within a given intercostal field, so that the quantification of the cross-area could thus be unequivocally attributed to the colonisation mode.

Surface hyphae were clearly absent from cv. Müller-Thurgau, the American species *V. riparia* and *V. rupestris*, and the Siberian species *V. amurensis*. However, surface hyphae were strongly present in the Asian species *V. jacquemontii*, *V. coignetiae* (Fig. 7C) and *V. ficifolia* and in the wild European *V. sylvestris* Ketsch. Surface hyphae were also noted to a certain extent in the hybrid cv. Merzling. The frequency of intercostal fields, where surface growth was observed, varied inversely with the frequency of intercostal fields where the pathogen developed inside the leaf (Fig. 7D).

We statistically tested the relative contributions of host accession *versus* inoculum to the observed indicators of

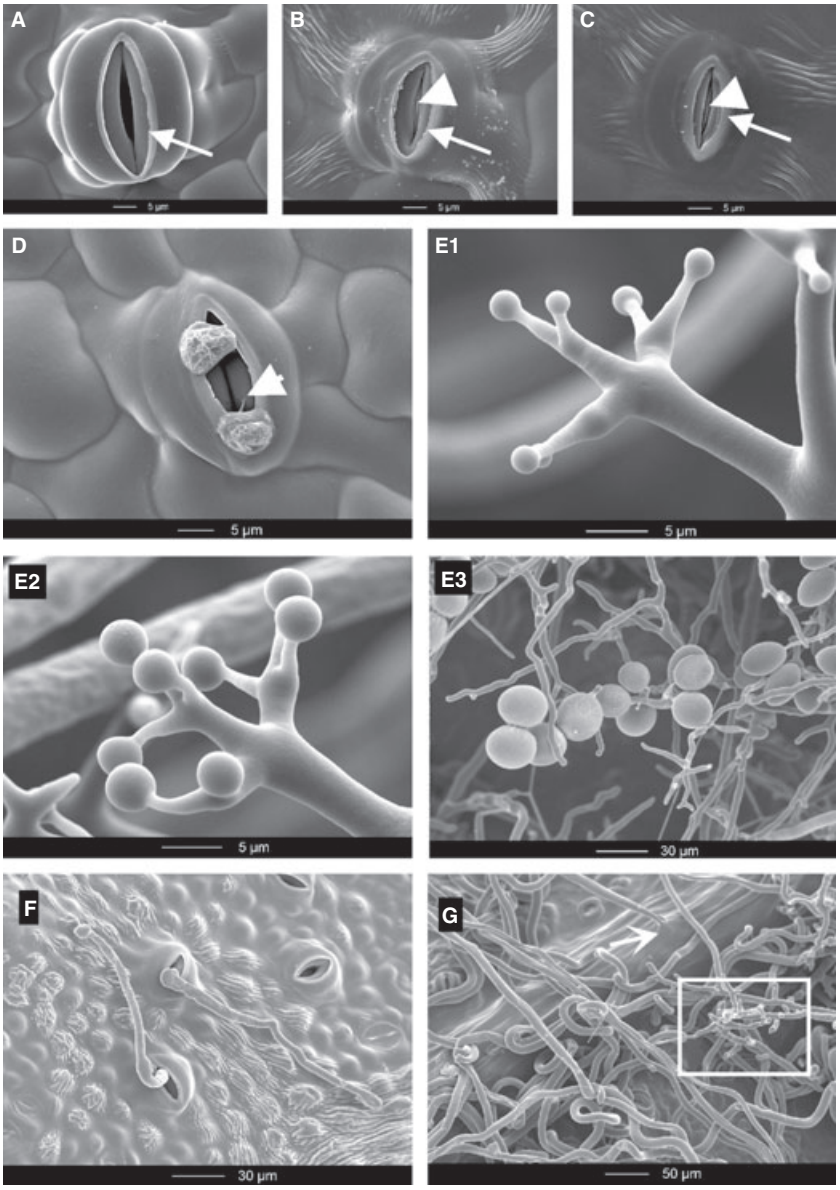

Fig. 3. Guard cell morphology and infection as visualised by LT-SEM. A–C: View of open guard cells of the grapevine cv. Müller-Thurgau (A) *versus Vitis riparia* (B) and *Vitis rupestris* (C) prior to infection. White arrows indicate the outer cuticular rim, and white arrowheads indicate the inner cuticular rim. D–G: Early (D) and late (E1–E3) infection in the grapevine cv. Müller-Thurgau. E1–E3 Developmental sequence illustrating the formation of sporangiophores and the formation of fine lateral hyphae emerging from the more solid sporangiophorous hyphae. For comparison, infection in the wild European *Vitis vinifera* ssp. *sylvestris* (F) and Asian *Vitis jacquemontii* (G) are shown. White box in G shows aberrant sporulation structures on *V. jacquemontii*. White arrowhead in D shows a dehydrated germ tube.

colonisation. To compare more than two samples with respect to the influence of qualitative, ordinal scaled variables (such as host accession and inoculum batch), we used the Kruskal–Wallis test as a non-parametric version of MANOVA. For all three indicators (infected area as a proportion of total area, colonisation intensity for a given infection event, and area of surface mycelium), the variance was predominantly caused by the cultivar, whereas the inoculum batch (and thus also the season) did not contribute relevantly to the variance. In the case of the infected area, the calculated values were 0.62 for the influence of the source of inoculation ($P = 0.987$), and 42.5 for the influence of the host genotype ($P < 0.0001$); in the case of colonization intensity, the values were 0.80 for the influence of the source of inoculation ($P = 0.977$) and 42.3 for the influence of the host genotype ($P < 0.0001$); and in the case of surface growth, the values were 0.62 for the influence of the source of inoculation ($P = 0.987$) and 43.3 for the influence of the host genotype ($P < 0.0001$), with P representing the probability of the null hypothesis that the differences arose randomly and independently of the respective factor.

DISCUSSION

Stomatal targeting depends on the host species

In previous work, we demonstrated that several aspects of early *P. viticola* development are clearly regulated by host factors (Kiefer *et al.* 2002): (i) the formation of zoospores

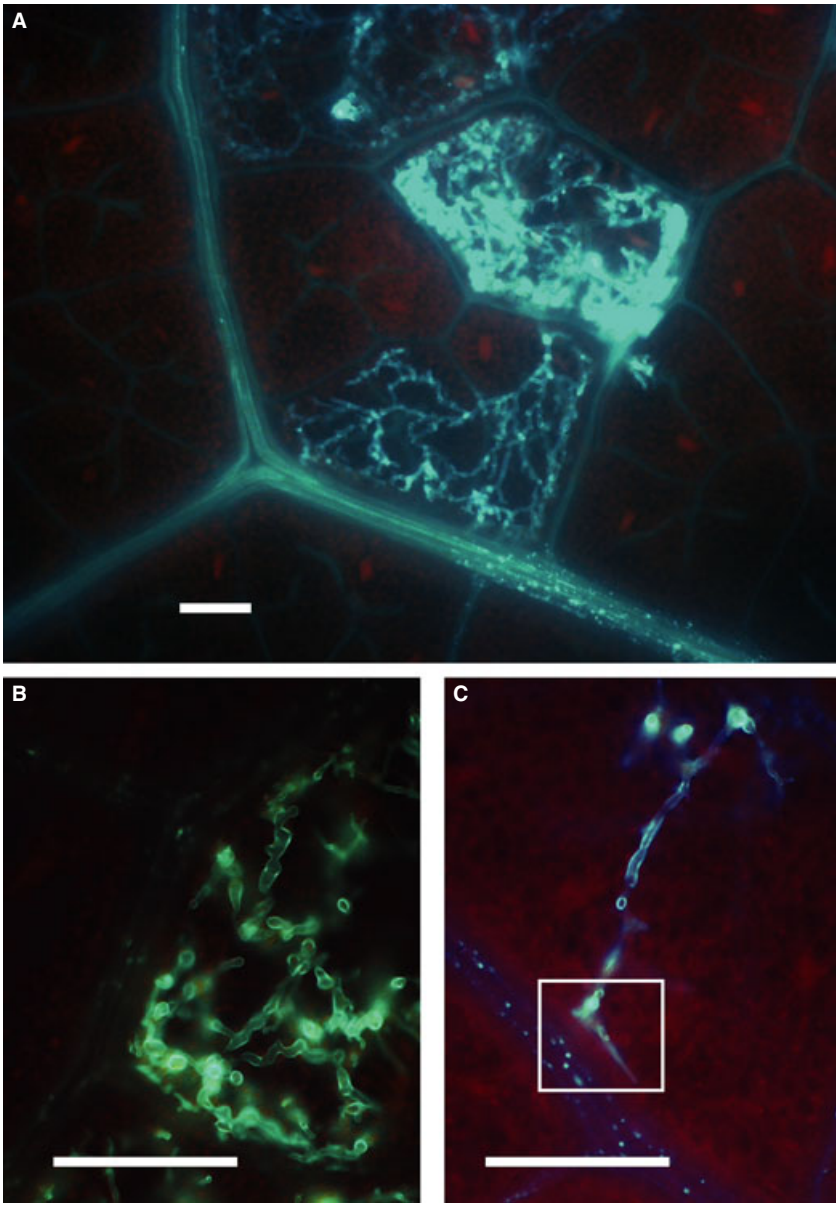

Fig. 4. Successful colonisation on a susceptible host (grapevine cv. Müller-Thurgau) visualised by aniline blue staining 72 h after inoculation. A: Overview of an infected intercostal field. B: Close-up of penetrated hyphae. C: Barrier response of an extending hyphae at the leaf vein.

within the mature sporangia was accelerated on the surface of the leaf of a compatible host genotype relative to a host-free system (Kiefer *et al.* 2002); and (ii) the zoospores track the stomata very efficiently within a few minutes after their release from the sporangia, and are guided by unknown host factors. When stomatal closure was induced by administering abscisic acid through the petiole, the accumulation of zoospores at the stomata was impaired in a concentration-dependent manner, which argues strongly for active taxis guided by a factor released from open stomata. The comparison of infection patterns between different *Vitis* host species indicates that, in addition to other mechanisms such as a hypersensitive response, production or incorporation of toxic compounds, callose formation and cell wall reinforcement, these host signals are targets of evolutionary change (Busam *et al.* 1997; Kortekamp *et al.* 1997; Gindro *et al.* 2003; Hamiduzzaman *et al.* 2005).

In the infection pattern where hyphae are formed on the surface of the leaf, stomatal targeting was strongly impaired. Here, the zoospores attached either to protruding structures, such as leaf veins or trichomes, or somewhere on the leaf surface (Figs 3G, 6 and 7C). Interestingly, this 'tracking failure' did not result in immediate developmental arrest, but was followed by extensive formation of surface hyphae, which, in some cases, *e.g.* on *V. jacquemontiii*, (Figs 6A–E and 7C), produced a mycelium covering large areas of the leaf. With

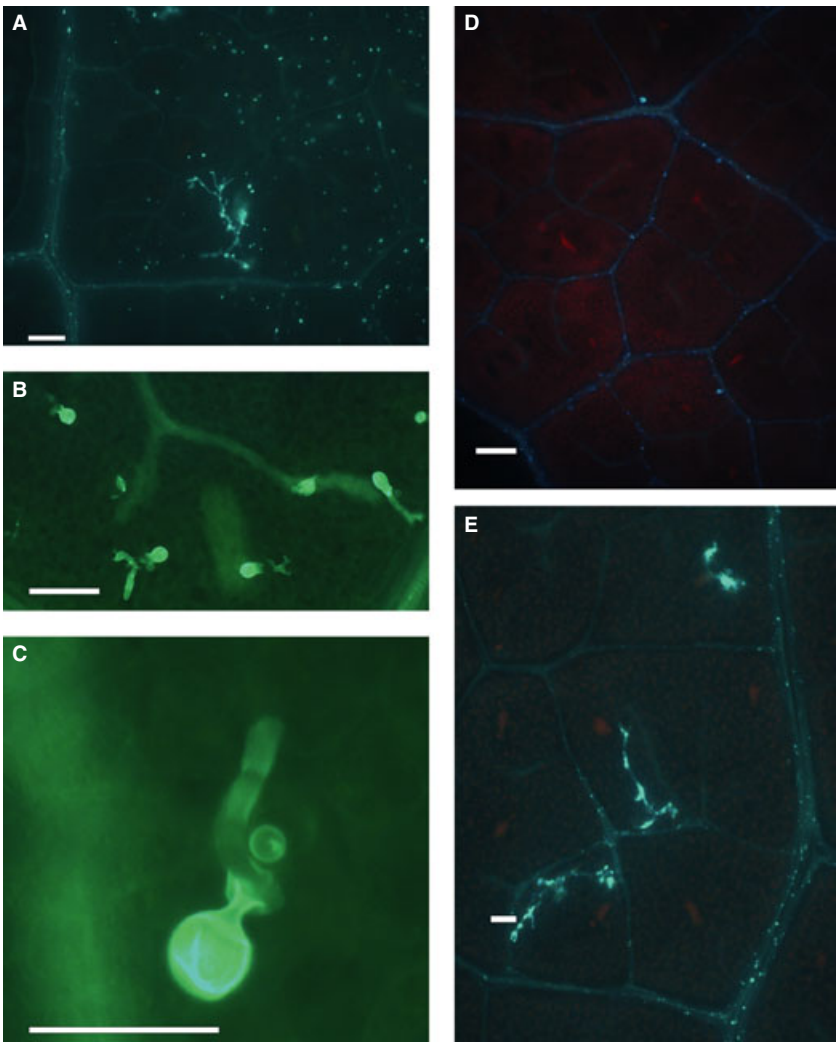

Fig. 5. Inhibited colonisation on a resistant host visualised by aniline blue staining 72 h after inoculation. A–C: Siberian species *Vitis amurensis*. A: Overview of an infected intercostal field in the Siberian species *V. amurensis*. Note the numerous fluorescent dots. B, C: Close-ups at higher magnification demonstrate that these fluorescent dots represent residual mycelia that have been arrested at an early stage of development. D: North American *Vitis riparia*. E: North American *Vitis rupestris*.

the exception of the wild European *V. vinifera* Ketsch, which represented an intermediate situation, these mycelia did not penetrate through the guard cells into the mesophyll. Although the initial development of this mycelium appeared to be fairly normal, the later development was clearly aberrant. Rather than producing the sporangiophores typical for infection of susceptible hosts (Fig. 3E1–E3), the mycelium developed whorls of fine, branched hyphae (Fig. 6F, white box). Similar fine, branched hyphae that were contiguous with sporangia (Fig. 3E1–E5) were observed after infection in the susceptible cv. Müller-Thurgau. The hyphae of the surface mycelium observed on *V. coignetiae*, *V. ficifolia*, *V. quinquangularis* and *V. jacquemontii* formed no septae, which is typical for the oomycetes (Dick 2001). We tested the possibility that the surface hyphae arose from fungi other than *P. viticola* by incubating parallel control discs that had not been inoculated with *P. viticola*. Over more than 3 years of experimentation, we never observed any mycelia or hyphae on these controls. In addition, we performed control experiments, where sporangia derived from axenically cultivated plantlets were infected in parallel to *V. coignetiae*, *V. ficifolia* and the susceptible cv. Müller-Thurgau. Since the same inoculum produced a surface mycelium on the two host species from Asia, but the typical mesophyll colonisation pattern in the susceptible cv. Müller-Thurgau, the differential behaviour cannot be attributed to a contaminant fungus. Moreover, the lack of septate hyphae in this surface mycelium is a typical feature of *P. viticola* (Kortekamp 2005), further supporting the conclusion that this surface mycelium is in fact formed by *P. viticola* and not caused by contamination with true fungi. Moreover, the NL and LR regions of the large subunit of the 25–28S RNA from this surface were identical to those from the source inoculum (S. Schröder, W. Wilcox & P. Nick, unpublished data). The most conclusive evidence, however, is the fact that the development of these mycelia can be traced back to zoospores that failed to attach at the guard cell (Fig. 6A–E). Such extensive expansion cannot occur without externally-provided energy. It remains to be

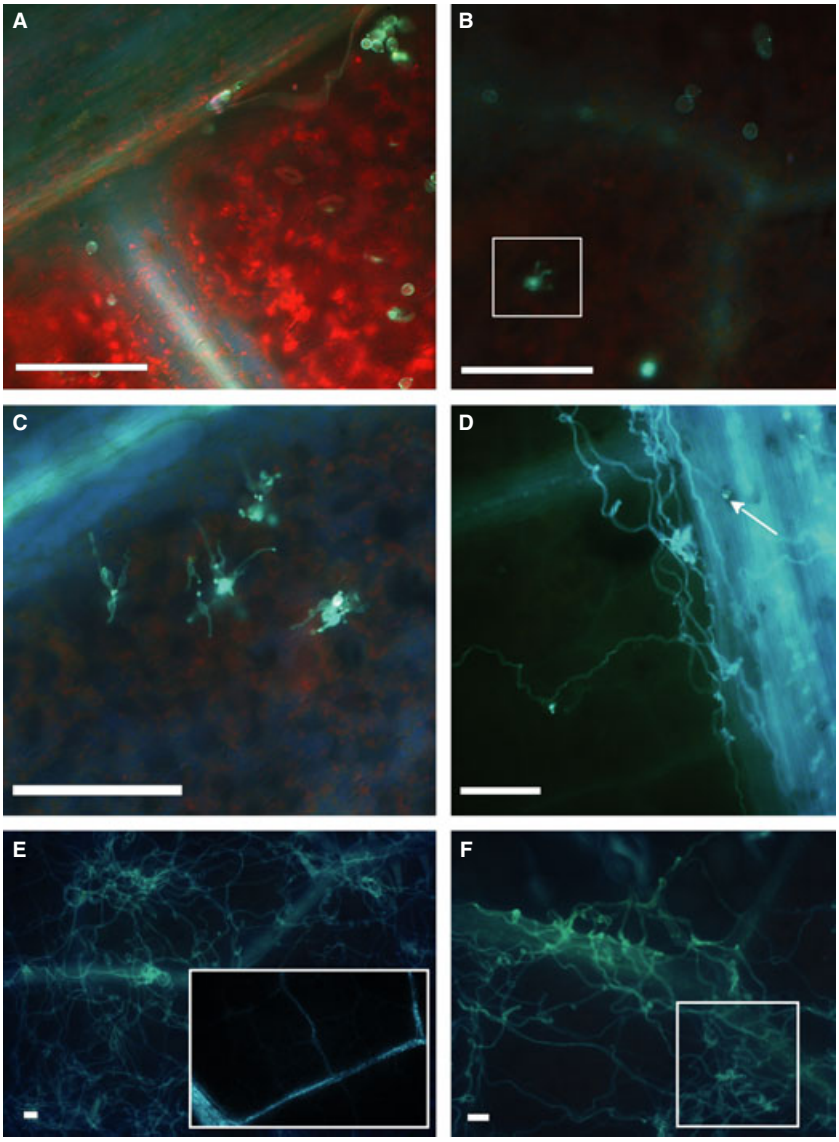

Fig. 6. Aberrant pathogen development with formation of surface hyphae visualised by aniline blue staining at different time points after inoculation. A–E: Different infection stages observed on the Asian host *Vitis jacquemontii* at 4 (A), 8 (B), 12 (C), 36 (D) and 72 (E) h after infection. Arrow in D shows a zoospore attached to a vein. Inset in E shows a negative control of *V. jacquemontii* that had been incubated for 72 h without inoculation. F: Wild European *V. sylvestris* Ketsch. Size bar 20 μm.

elucidated how the hyphae that do not penetrate through the stomata can withdraw the necessary carbohydrates from the apparently intact leaf, and we know of no case of such a saprotrophic Peronosporomycete. However, it should be mentioned that hyphae of the related *Peronospora viciae* have been shown to be capable of direct photoassimilate uptake (Clark & Spencer-Phillips 1993) and can accumulate glucose *in vitro* (El-Gariani & Spencer-Phillips 2004). However, in our experiments these mycelia were observed on leaf discs under artificial conditions with very high humidity, *i.e.* under artificial conditions. Recently, Díez-Navajas *et al.* (2008) described encysted zoospores with a wandering germ tube near leaf veins on the surface of *Lactuca sativa* inoculated with *P. viticola*, probably due to a weaker stomatal targeting in this non-host plant. It remains to be tested whether the misplacement of zoospores will also result in surface mycelia under field conditions. Despite this *caveat* concerning the occurrence of surface mycelia under field conditions, we are convinced that the mycelium observed on the East Asian host species originates from *P. viticola* that fail to produce sporangia.

The wild European *V. vinifera* Ketsch represents an interesting intermediate state between the abortive fungal development observed on the East Asian species and susceptibility typical for cultivated grapevines. Here, although many zoospores initiate formation of a mycelium on the surface of the leaf, there are at least some zoospores that can track the stomata, culminating in successful penetration through the substomatal cavity. Thus, the tracking ability of these spores, although reduced as compared to the susceptible cv. Müller-Thurgau, is still preserved, as evidenced by the formation of a germ tube that grows directionally towards the guard cell (Fig. 3F).

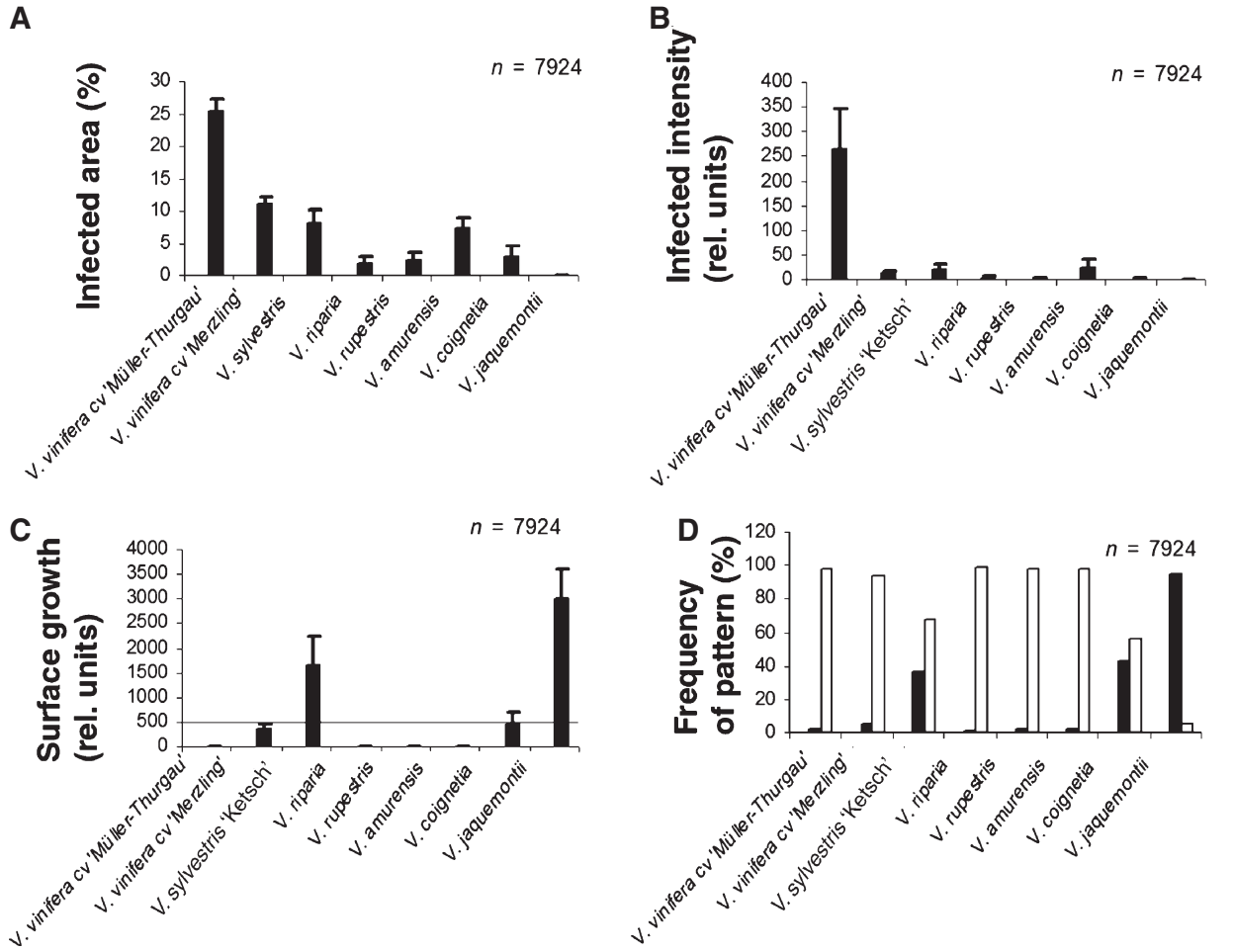

Fig. 7. Quantitative analysis of host–pathogen interaction in different *Vitis* species. A: Infected area (as % of total area). B: Colonisation intensity (relative units). C: Surface growth without mesophyll colonisation (relative units). n = number of evaluated intercostal fields. D: Frequency of intercostal fields with surface growth without mesophyll colonisation (black bars) *versus* frequency of intercostal fields with successful colonisation of the mesophyll (white bars).

It seems that in wild *V. vinifera* Ketsch the signal responsible for the attraction of zoospores to the guard cell is less effective than in cv. Müller-Thurgau, such that zoospores are more likely to attach at topologically similar structures, comparable to the situation in the East Asian species. However, this host signal still seems to be sufficiently active to guide the growth of the germ tube even from relatively distant locations on the leaf.

In the species where colonisation is inhibited, it seems to be primarily the development of primary hyphae and subsequent haustoria formation that is arrested, consistent with previous results (Langcake & Lovell 1980; Dai *et al.* 1995; Unger *et al.* 2007). In our studies, this was most evident for the Siberian species *V. amurensis*, where zoospores seem to track the stomata, attach around the guard cells and penetrate into the substomatal cavity with high efficiency (Fig. 7A), but are then unable to colonise the host efficiently (Fig. 7B). The situation in the American species *V. riparia, V. rupestris* and *V. californica* seems to be comparable, although here the number of primary infections is very low (Fig. 7A), and many spores are observed to attach at the leaf veins (Fig. 5D and E). It remains to be elucidated whether this is caused by impairment of stomatal targeting. The central difference in this response mode is the arrest of pathogen development shortly after penetration into the substomatal cavity, as recently described in detail for *V. rupestris* (Unger *et al.* 2007) and for *V. riparia*, *Muscadinia rotundifolia* (syn. *V. rotundifolia*) and several non-host taxa (Díez-Navajas *et al.* 2008). This indicates that the North American host species (as well as the Siberian species *V. amurensis*) are endowed with efficient mechanisms to recognise and to stop attacks by *P. viticola*.

A role for the inner cuticular rim in plant defence?

In all species studied in the present work, the inhibition of colonisation was always correlated with the presence of

an inner cuticular rim at the transition between the substomatal cavity and the stoma *sensu strictu* (Figs 2 and 3 Table 1). This inner cuticular rim was absent in the East Asian species, where *P. viticola* formed mycelia on the leaf surface, thereby refuting the hypothesis that this inner cuticular rim somehow impairs zoospore tracking by inhibiting the release of the guiding signal through the stomata. On the other hand, the fact that all species that are able to arrest the initiated colonisation of the mesophyll are endowed with this inner cuticula rim (Table 1) suggests that this relationship is of functional significance. It also seems unlikely that this protrusion represents a xeromorphic adaptation, because the majority of species in which it is observed originate from relatively humid habitats such as riverbanks (http://www.ars-grin.gov/). Thus, although the inner cuticular rim is probably not involved in the suppression of zoospore tracking, it can be interpreted in the context of plant defence. In the North American species *V. rupestris, V. riparia* and *V. californica* and in the Siberian species *V. amurensis*, where this inner cuticular rim is present, zoospores can attach at the stomata but subsequent development is suppressed at an early stage (Fig. 5). The American species presumably have undergone coevolution with *P. viticola*. The inner cuticular rim might therefore be interpreted as a preformed resistance mechanism evolved as a consequence of the arms race between the host plant and the pathogen. A plausible interpretation of the occurrence of this preformed barrier in *V. amurensis* may be the presence of a closely related Peronosporomycete that also penetrates the host tissue *via* the stomata. In fact, Grünzel (1959) mentioned *P. amurensis* as a pathogen of East Asian *Vitis* species. The European taxa (cv Müller-Thurgau belonging to the taxon *V. vinifera* ssp. *sativa* as well as the ancestral wild European species *V. vinifera* ssp. *sylvestris*) that are susceptible do not possess this inner cuticular rim. We therefore hypothesise that the inner cuticular rim might represent an adaptation to impair or at least delay growth of the germ tube through the stomata in a way similar to the callosic plugs that have been shown to contribute to defence against fungal penetration in *Vitis* (Kortekamp *et al.* 1997; Gindro *et al.* 2003; Hamiduzzaman *et al.* 2005), and in other systems (Nishimura *et al.* 2003). It should be considered, however, that (1) the data presented in this study have been obtained with leaf discs, the situation in the field might differ, and (2) in several cases only one accession per host species was employed and, especially for the evolutionary advanced situation in North America, considerable intraspecies variation is to be expected. However, we will soon publish a more extensive infection study involving accessions from all known wild *Vitis* species, along with data on molecular phylogeny of these species that confirm the biogeographical context of the infection patterns reported in the present work.

The hypothesis that the inner cuticular rim represents a preformed defence response could be tested experimentally when the time courses in the expression of defence genes are compared to those of host colonisation in pairs of closely related species that differ in the presence of this guard cell structure. If the inner cuticular rim contributes to defence, the colonisation would proceed more slowly in relation to the induction of defence genes.

ACKNOWLEDGEMENTS

The competent and highly motivated support of Joachim Daumann (Botanical Garden, Karlsruhe University) in the cultivation and propagation of the different *Vitis* species is gratefully ackowledged. We also gratefully acknowledge the support of the USDA National Clonal Germplasm Repository, University of California-Davis (USA) who kindly provided some wild *Vitis* species.

REFERENCES

Busam G., Junghans K.T., Kneusel R.E., Kassemeyer H.H., Matern U. (1997) Characterization and expression of Coffeoyl-coenzyme A 3-*O*-methyltransferase proposed for the induction for the induced resistance response of *Vitis vinifera* L. *Plant Physiology*, **115**, 1039–1048.

Clark J.S.C., Spencer-Phillips P.T.N. (1993) Accumulation of photoassimilate by *Peronospora viciae* (Berk.) Casp. and leaves of *Pisum sativum* L.: Evidence for nutrient uptake via intercellular hyphae. *New Phytologist*, **124**, 107–119.

Dai G.H., Andary C., Mondolot-Cosson L., Boubals D. (1995) Histochemical studies on the interaction between three species of grapevine, *Vitis vinifera*, *V. rupestris* and *V. rotundifolia* and the downy mildew fungus *Plasmopara viticola*. *Physiological Molecular Plant Pathology*, **46**, 177–188.

Dick M.W. (2001) The Peronosporomycetes. In: McLaughlin D.J., McLaughlin E.G., Lemke P.A. (Eds), *The Mycota VII Part A. Systematics and Evolution*. Springer, Berlin Heidelberg: 39–73.

Dick M.W. (2002) Towards an understanding of the evolution of the downy mildews. In: Spencer-Phillips P.T.N., Gisi U., Lebeda A. (Eds), *Advances in Downy Mildew Research, Vol. 1*. Kluwer, Dordrecht: 1–59.

Díez-Navajas A.M., Wiedemann-Merdinoglu S., Greif C., Merdinoglu D. (2008) Nonhost versus host resistance to grapevine downy mildew, *Plasmopara viticola*, studied at the tissue level. *Phytopathology*, **98**, 776–780.

El-Gariani A., Spencer-Phillips P.T.N. (2004) Benzothidiazole-induced resistance to *Plasmopara halstedii* (Farl.) Berl et de Toni in sunflower. In Spencer-Phillips P.T.N., Jeger P. (Eds), *Advances in Downy Mildew Research, Vol. 2*. Kluwer, Dordrecht: 265–273.

Gindro K., Pezet R., Viret O. (2003) Histological studies of the response of two *Vitis vinifera* cultivars (resistant and susceptible) to *Plasmopara viticola* infections. *Plant Physiology & Biochemistry*, **41**, 846–853.

Grünzel H. (1959) Zur biologischen Differenzierung des Falschen Mehltaus der Weinrebe (*Peronospora viticola* deBary). *Zentralblatt Bakteriologie II*, **112**, 454–472.

Guggenheim R., Düggelin M., Mathys D., Grabski C. (1991) Low-temperature SEM for the detection of fungicide activity. *Journal of Microscopy*, **161**, 337–342.

Hamiduzzaman M.M., Jakab G., Barnavon L., Neuhaus J.M., Mauch-Mani B. (2005) β-Aminobutyric acid-induced resistance against downy mildew in grapevine acts through the potentiation of callose formation and jasmonic acid signalling. *Molecular Plant Microbe Interaction*, **18**, 819–829.

Kiefer B., Riemann M., Büche C., Kassemeyer H.H., Nick P. (2002) The host guides morphogenesis and stomatal targeting in the grapevine pathogen *Plasmopara viticola*. *Planta*, **215**, 387–393.

Kortekamp A. (2005) Growth, occurrence and development of septa in *Plasmopara viticola* and other members of the Peronosporaceae using light and epifluorescence microscopy. *Mycology Research*, **109**, 640–648.

Kortekamp A., Wind R., Zyprian E. (1997) The role of callose deposits during infection to downy mildew-tolerant and two susceptible *Vitis* cultivars. *Vitis*, **36**, 103–104.

Langcake P., Lovell P.A. (1980) Light and electron microscopical studies on the infection of *Vitis* ssp. by *Plasmopara viticola*, the downy mildew pathogen. *Vitis*, **19**, 321–337.

Müller K., Sleumer H. (1934) Biologische Untersuchungen über die Peronosporakrankheit des Weinstocks mit besonderer Berücksichtigung ihrer Bekämpfung nach Inkubationsmethode. *Zeitschrift für Wissenschaftliche Landwirtschaft*, **79**, 509–576.

Müller T., Guggenheim R., Düggelin M., Scheidegger C. (1991) Freeze fracturing for conventional and field emission low-temperature scanning electron microscopy: the cryo-scanning unit SCU. *Journal of Microscopy*, **161**, 73–83.

Nishimura M.T., Stein M., Hou B.-H., Vogel J.P., Edwards H., Somerville S.C. (2003) Loss of a callose synthase results in salicylic acid-dependent disease resistance. *Science*, **301**, 969–972.

Riemann M., Büche C., Kassemeyer H.H., Nick P. (2002) Microtubules and actin microfilaments guide the establishment of cell polarity during early development of the wine pathogen *Plasmopara viticola*. *Protoplasma*, **219**, 13–22.

Unger S., Büche C., Boso S., Kassemeyer H.H. (2007) The course of the colonization of two different *Vitis* genotypes by *Plasmopara viticola* indicates compatible and incompatible host–pathogen interactions. *Phytopathology*, **97**, 781–786.

Vercesi A., Tornaghi R., Burruano S.S., Faoro F. (1999) A cytological and ultrastructural study on the maturation and germination of oospores of *Plasmopara viticola* from overwintering vine leaves. *Mycological Research*, **103**, 193–202.